Exciton Spin Relaxation in Semiconductor Quantum Wells: The Role of Disorder

H. Nickolaus, H.-J. Wünsche, and F. Henneberger
Institut für Physik, Humboldt-Universität zu Berlin, Invalidenstrasse 110, 10115 Berlin, Germany
(Received 5 May 1998)

Ultrafast pulse measurements on high-quality (Zn, Cd)Se/ZnSe quantum wells yield the very surprising result that the decay of the exciton spin transients after resonant excitation with circularly polarized light is even faster than the exciton dephasing time. We demonstrate that this fact is a direct consequence of (alloy) disorder which gives rise to a kind of inhomogeneous broadening and associated interference effects for spin dynamics across the band of localized exciton states. [S0031-9007(98)07100-2]

PACS numbers: 78.66.Hf, 71.35.Gg, 73.20.Dx

Below band-gap optical excitation of a semiconductor by circularly polarized light creates excitons with definite spin orientation. During recent years, much interest has been focused on the spin relaxation of excitons in quantum well (QW) structures [1–8]. However, despite these efforts, the understanding of the spin reversal in two dimensions is far from being complete. The numbers reported for the spin relaxation time are strongly sample dependent—even for QW's of nominally the same design—and scatter between 1 and 220 ps. These divergent findings suggest that disorder being an inherent feature of QW's (alloy fluctuations, interface roughness, ...) plays an important role also in the exciton spin dynamics. Though being an obvious conclusion, this aspect has not yet been explicitly elaborated.

In this Letter we present a study of the exciton spin dynamics in ternary QW's, using in the experimental part (Zn, Cd)Se/ZnSe. In comparison with GaAs/(Ga, Al)As QW's, on which most of the previous work has been done, II-VI structures offer a number of advantages. First, the big exciton binding energy allows one to tolerate a larger disorder-induced inhomogeneous broadening of the exciton without affecting the internal electron-hole relative motion. Second, the electron-hole exchange interaction is distinctly stronger, enabling thus a direct spectral measurement of the characteristic energies involved in the spin relaxation. Third, exciton and biexciton transitions are well separated as the result of the larger biexciton binding energy.

The prototype (Zn, Cd)Se/ZnSe QW structure used in the present study consists of 5 QW's of 5 nm thickness and a Cd mole fraction of 13%, separated by 85 nm wide ZnSe barriers. Its excitonic properties are well known from previous studies using various experimental techniques [9]. The exciton and biexciton binding energies are 33.6 and 10.0 meV, respectively. We have performed pump-probe and degenerated four-wave mixing (DFWM) measurements. Intense 200 fs pulses from a Ti:Sa oscillator-amplifier system generate a white-light continuum, used as the probe beam, and pump an optical parametric amplifier (OPA). The signal wave of the OPA was tuned to the heavy hole (HH) exciton resonance and served as the pump beam as well as for the DFWM setup. The polarization control of the beams was better than 100:1. All measurements were carried out at $T = 5$ K.

Before coming to the spin relaxation itself, we first present data which are of importance for the later discussion. Generally, in the presence of disorder, there is no translational symmetry in the QW plane. The exciton (as well as biexciton) energies exhibit a distribution, where each energy belongs to a certain in-plane location of the particle, referred to as "site" in what follows. In the present case, characterized by a ternary (Zn, Cd)Se QW, alloy fluctuations defining the main disorder source provide a site density in the 10^{11} cm^{-2} range [9]. The inhomogeneous width of the HH exciton absorption band (see inset Fig. 2) is 8.8 meV (FWHM). Figure 1 depicts the polarization decay at the HH exciton line center, taken from time-integrated DFWM measurements for a set of pulse fluxes ξ. The latter allows the definition of the low-density

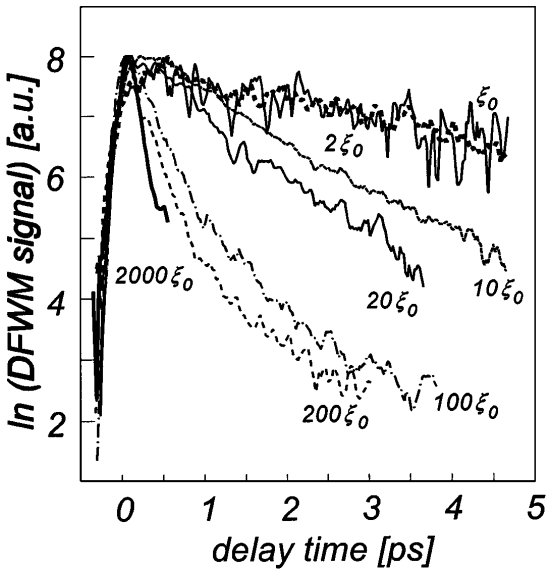

FIG. 1. Time-integrated DFWM transients at the HH exciton line center for different densities ($\xi_0 \approx 100$ nJ/cm^2).

 0031-9007/98/81(12)/2586(4)$15.00

regime with an exciton dephasing time τ_2 being excitation-density independent. The data yield a constant value of $\tau_2 = 14$ ps for $\xi < 200$ nJ/cm^2, controlled by scattering on impurities or imperfections [10]. There is a slight variation of τ_2 by a factor of 1.4 across the exciton band with shorter times on the high-energy side. The homogeneous exciton width $\Gamma_{\text{hom}} = 2\hbar/\tau_2$ of about 100 μeV is thus 2 orders of magnitude smaller than the inhomogeneous broadening. On the other hand, the exciton binding energy is roughly 1 order of magnitude beyond the energy scale of the disorder, justifying the in-plane localization in terms of the exciton center-of-mass (c.m.) motion.

The HH exciton state consists of four levels with total angular momentum $|\pm 1\rangle$ and $|\pm 2\rangle$, the latter being optically forbidden (dark excitons). The degeneracy between the two angular momenta is lifted by the on-diagonal electron-hole exchange interaction [11], shifting the optically active states to higher energies. For the present (Zn,Cd)Se QW's, a splitting of 0.5 meV has been deduced from magneto-optical data, while time-resolved photoluminescence (PL) measurements have yielded that the conversion of an allowed state in a dark exciton takes place on the nanosecond time scale (at low temperature and no magnetic field) [12]. This conversion involves a single-particle spin flip, commonly attributed to the hole, that is, from $|\pm 1\rangle$ to $|\mp 2\rangle$. In this Letter, we focus on the direct exciton spin reversal, controlling the relaxation among the optically allowed $|\pm 1\rangle$ states. In time-resolved PL under resonant excitation, there is, however, no significant polarization memory observable within the experimental time resolution of 10 ps. We have therefore performed nonlinear absorption ($\Delta\alpha$) measurements with sup-ps time resolution. The excitation level was adjusted in accordance with the low-density regime of the DFWM study. The concept of the experiment is as follows: A σ^+ polarized pump pulse prepares resonantly spin-up excitons on a small fraction ($<10^{10}$ cm^{-2}) of localization sites. For a σ^- probe photon, the absorption of these sites is blocked ($\Delta\alpha = -\alpha_0$), whereas stimulated emission occurs for σ^+ polarization ($\Delta\alpha = -2\alpha_0$). Therefore, plotting the difference of the nonlinear absorption signals in the two polarization configurations versus pump-probe delay (see Fig. 2), the degree of spin relaxation in the exciton system becomes directly visible. In addition to changes at the exciton resonance, we also observe pronounced induced absorption features due to biexcitons [13]. As already mentioned, they are clearly separated from the exciton absorption and have thus no misleading influence on the spin dynamics. The plot in Fig. 2 is for a detection energy on the low-energy exciton flank as marked in the inset, where the linear absorption is depicted for reference. In view of the 20 meV spectral pulse width, the excitation is almost homogeneous across the site distribution. We do not observe any substantial change of the transients when tuning the detection over the absorption band. The most striking feature of our finding is, however, that the

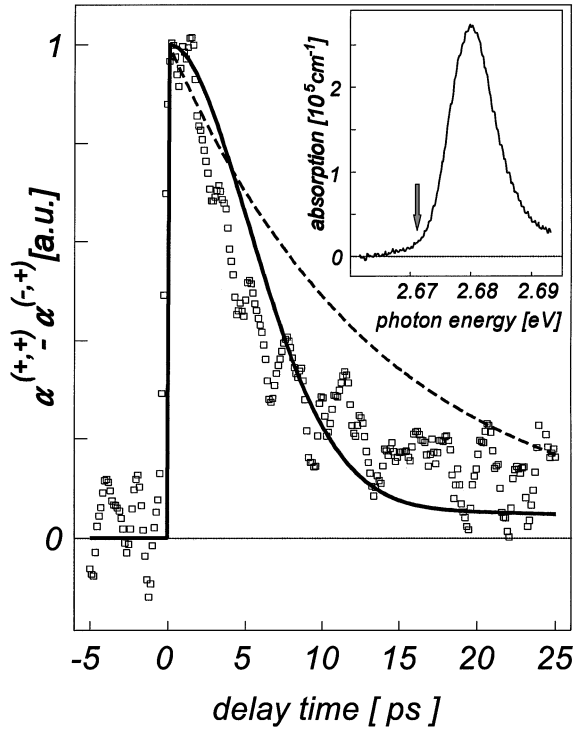

FIG. 2. Difference of the nonlinear absorption in the $\sigma^{+,+}$ and $\sigma^{+,-}$ configurations (squares). Dashed line: Single-exponential decay according to the dephasing time of 14 ps for comparison. Solid line: Fit according to the model described in the text. Inset: Linear absorption.

spin relaxation is apparently faster than the polarization dephasing, defining the earliest scattering events of the exciton. In what follows, we demonstrate that this is a direct consequence of disorder.

Maialle *et al.* [4] have shown that the exciton spin flip in QW's is related to the long-ranged part of the electron-hole exchange interaction. The off-diagonal terms $H_{\text{LR}}^{(\pm)}$ give rise to a coupling between the spin-up and spin-down states. Thus, after preparing the system in a well-defined spin state by a circularly polarized light pulse, the exciton spins start to precess coherently with a certain frequency. Scattering on phonons or impurities randomizes this precession so that the photoimprinted average spin vanishes more and more with increasing time after excitation. In an ideal QW with full translational symmetry perpendicular to the growth axis, a finite c.m. (in-plane) momentum $\boldsymbol{k}$ on the exciton is required, as the long-ranged exchange coupling is zero at $\boldsymbol{k} = 0$. In the present case of spatially confined states, each exciton comprises a set of $\boldsymbol{k}$ vectors, distributed according to the Fourier transform $\Phi(\boldsymbol{k})$ of its c.m. wave function. The coupling between spin-up and spin-down states for a given site is evaluated by averaging the matrix elements of the ideal QW [4] with this Fourier transform, providing

$$H_{\text{LR}}^{(\pm)} = \frac{3}{16}\,\pi a_x^3 |\varphi_{1s}(0)|^2 \Delta E_{\text{LT}} K_{\text{site}}^{(\pm)} \qquad (1)$$

(a_x: bulk exciton Bohr radius; ΔE_{LT}: bulk longitudinal-transverse splitting; φ_{1s}: QW wave function of electron-hole relative motion), where

$$K_{\mathrm{site}}^{(\pm)} = \int d^2\boldsymbol{k} |\phi(\boldsymbol{k})|^2 \frac{f(k)}{k} (k_x \pm i k_y)^2. \qquad (2)$$

($k^2 = k_x^2 + k_y^2$) represents an effective c.m. momentum, characteristic of this site. The form factor $f(k)$ [4] is approximated by $f(0) = 1$ in the explicit calculations presented below. We emphasize that $K_{\mathrm{site}}^{(\pm)}$ vanishes for a radially symmetric site with Φ being a function of k only. Solution of the Bloch equations yields, for the exciton net spin on a single site,

$$S_z(t) = \frac{1}{2}\left[\left(1 + \frac{\tau_+\tau_-}{\tau_2(\tau_- - \tau_+)}\right)e^{-t/\tau_-} + \left(1 - \frac{\tau_+\tau_-}{\tau_2(\tau_- - \tau_+)}\right)e^{-t/\tau_+}\right] \qquad (3)$$

with the (complex) time constants

$$\frac{1}{\tau_\pm} = \frac{1}{2\tau_2}(1 \pm \sqrt{1 - 4\Omega^2\tau_2^2}),$$
$$\hbar^2\Omega^2 = 4H_{\mathrm{LR}}^{(+)}H_{\mathrm{LR}}^{(-)}. \qquad (4)$$

In the limit $2\Omega\tau_2 \ll 1$, the spin transient is a single-exponential decay with characteristic time $\tau_{\mathrm{SR}} = 1/\Omega^2\tau_2$ much longer than τ_2 (damping regime). Conversely, for $2\Omega\tau_2 \gg 1$, oscillations of frequency Ω occur, weakly exponentially damped with $\tau_{\mathrm{SR}} = 2\tau_2$ (oscillatory regime). None of these predictions, long spin relaxation time τ_{SR} or oscillating signal, are observed experimentally. In contrast, our apparent τ_{SR} is even about 2 times shorter than τ_2. However, the experimental data represent an average over the ensemble of sites, each of which may have a different value of Ω. In the spectral domain, the off-diagonal exchange coupling manifests as an energy splitting of $\hbar\Omega$ between the optically allowed exciton states. In high-resolution magneto-optical measurements [12], a mean value of $\hbar\Omega \leq 100\ \mu$eV has been found for the present QW structures, yielding $2\Omega\tau_2 \approx 4$. The actual spin response will thus critically depend on how this mean value is distributed over the site ensemble, which is elaborated next. Our considerations are based on two main assumptions. First, following Wilkinson *et al.* [14], we use for the random exciton c.m. potential the expression

$$V(\boldsymbol{r}) = \int d^2\boldsymbol{r}' F(|\boldsymbol{r} - \boldsymbol{r}'|) w(\boldsymbol{r}'), \qquad (5)$$

where the white noise function $w(\boldsymbol{r})$ with $\langle w(\boldsymbol{r})\rangle = 0$ and $\langle w(\boldsymbol{r})w(\boldsymbol{r}')\rangle = \delta(\boldsymbol{r} - \boldsymbol{r}')$ represents the QW alloy disorder. A Gaussian $F(\boldsymbol{r}) = \sigma \exp(-r^2/l^2)/\sqrt{\pi}\, l^2/2$ is used for the convolution function. The two parameters are the variance σ and an effective correlation length l of the potential V. The second assumption is that the exciton c.m. wave function can be represented by the lowest eigenfunctions of the minima of this potential, treated in harmonic approximation. Choosing local coordinates for each minimum according to its principal axes, defined by the directions with the largest and smallest second-order derivatives V''_+ and V''_-, one finds

$$K_{\mathrm{site}} = \sqrt{K_{\mathrm{site}}^{(+)}K_{\mathrm{site}}^{(-)}} = \frac{3\sqrt{\pi}}{8}\sqrt{ME_0/\hbar^2}\,\frac{\delta E_0}{E_0}, \qquad (6)$$

where δE_0 and E_0 are the difference and sum of the zero-point energies $E_\pm = \hbar/2\,(V''_\pm/M)^{1/2}$ ($M = 0.6\ m_0$: exciton mass) of the two decoupled parabolas, respectively. For a potential of type (5), using dimensionless units, the density of minima with energy $f = V/\sigma$ and with second-order derivatives $f_\pm = l^2V''_\pm/\sigma$ along the principal axes is [14]

$$N(f, f_+, f_-) = \frac{f_+f_-(f_+ - f_-)}{16\pi^2 l^2}\exp\left\{-\frac{1}{2}\left[f^2 + \left(f + \frac{f_+ + f_-}{2}\right)^2 + \left(\frac{f_+ - f_-}{2}\right)^2\right]\right\}. \qquad (7)$$

It allows one to calculate the density of sites with exciton energy $E = \sigma f + E_0$ and effective momentum $K = K_{\mathrm{site}}$,

$$P\left(\frac{E}{\sigma}, K\right) = \int_0^\infty df_+ \int_0^{f_+} df_- N\left(\frac{E - E_0}{\sigma}, f_+, f_-\right) \times \delta(K - K_{\mathrm{site}}). \qquad (8)$$

For evaluating this distribution, we use $l \approx 9$ nm for the correlation length obtained by equating the theoretical density of minima $1/(2\pi l^2\sqrt{3})$ to the experimental site density of $10^{11}\ \mathrm{cm}^{-2}$. In the classical limit [14], the 8.8 meV absorption width corresponds to a variance of $\sigma \approx 4$ meV, which increases by about a factor of 2, when quantum narrowing [15] is accounted for. However, this uncertainty is not essential in the present context, since the numerical evaluation provides that P depends only smoothly on σ in the relevant parameter range. This is demonstrated by Fig. 3, where P is plotted for an exciton energy in the absorption tail, using two σ values above ($\triangle$) and below ($\bigcirc$) 8 meV. A prominent feature of these distributions is that a radially symmetric site occurs with very low probability, while the most likely geometry is $K \approx 2 \times 10^7\ \mathrm{m}^{-1}$, that is, $V''_-/V''_+ \approx 0.6$. The plots in Fig. 3, as well as further numerical data for other exciton energies and/or reasonable variations of the correlation length, can be surprisingly well fitted by the empirical formula

$$P(K) = \frac{K}{K_{\mathrm{max}}^2}\exp\left\{-\frac{3}{5}\left(\frac{K}{K_{\mathrm{max}}}\right)^{5/3}\right\}, \qquad (9)$$

where K_{max} defines the position of the maximum.

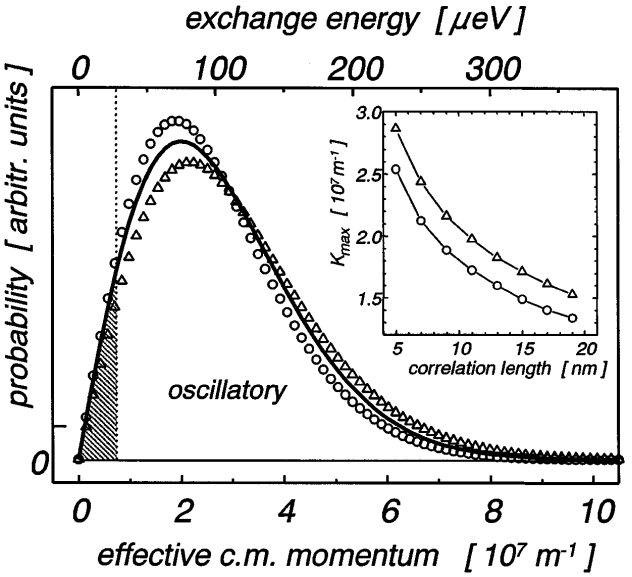

FIG. 3. Probability distribution of the effective c.m. momentum for $\sigma = 6\,\mathrm{meV}$ (○) and $\sigma = 10\,\mathrm{meV}$ (△) at an exciton energy $E = -1.5\sigma$ in the absorption wing ($l = 9$ nm). Solid line: Empirical fit according to formula (9) used for the calculation of the total spin decay in Fig. 2 with the upper horizontal scale for the precession energy. The vertical line defines $2\Omega\tau_2 = 1$. Hatched area marks those sites in the damping regime. Inset: Maximum of the distribution as a function of the correlation length l for otherwise unchanged parameters.

The distribution over K translates into a distribution over Ω, representing a kind of inhomogeneous broadening for the spin precession. The decay of the total spin seen in the experiment is therefore a superposition of all single-site transients $S_z(t)$ of given exciton energy weighted with the relative occurrence of precession frequency Ω among these sites. The only free parameter left in our approach is the QW prefactor in (1). When the longitudinal-transverse splitting and the Bohr radius of ZnSe is adopted ($\Delta E_{\mathrm{LT}} = 1.2$ meV, $a_x = 4.5$ nm), the best fit of the experimental data (solid line in Fig. 2) is yielded by a confinement factor $\pi a_x^3 |\varphi_{1s}(0)|^2 \approx 8.3\ \mathrm{nm} = 1.8 a_x$. The distribution of precession energies $\hbar\Omega$ underlying this fit is also depicted in Fig. 3. It is consistent with the 100 μeV average splitting in the spectral domain mentioned above. On the vast majority of sites, the spin is in the oscillatory regime. However, since precessing with different frequencies, interferences between the various single transients produce a monotonous decay of the total spin. The calculated overall signal resembles well the experimental data, exhibiting an initial fast drop with a subsequent slow tail, where the latter stems from those sites in the damping regime.

In the Cd mol fraction range ($<25\%$), where a description in terms of uncorrelated disorder is justified for (Zn,Cd)Se/ZnSe QW's, the site density and thus correlation length l do not vary substantially [9]. Generally, a larger value of l means weaker localization in real space and hence a less extended c.m. Fourier transform $\Phi(\boldsymbol{k})$. By this, the maximum $K_{\max}$ of the distribution function P is shifted to smaller K, as quantitatively depicted in the inset of Fig. 3. For a given scattering time τ_2 and QW parameters, this increases the amount of sites in the damping regime so that the slow component becomes more dominant in the total spin transients, whereas the opposite holds when the correlation length decreases.

In conclusion, we have demonstrated both experimentally and theoretically that disorder in a QW may cause an apparent very rapid spin decay, even faster than the polarization dephasing. This decay, however, is not related to a real relaxation of the individual exciton spins, but results from superposition of spin precessions with different frequencies. It is thus clear that samples with different disorder may exhibit largely varying spin transients. Our explicit analysis is based on alloy disorder in a ternary QW. This kind of spin relaxation scenario is, however, a general feature of excitons in structures with size or shape fluctuations (e.g., quantum dots) when the condition $\Gamma_{\mathrm{in}} \gg \hbar\Omega > \hbar/\tau_2$ is met.

The authors thank Michael Rabe for growth of the samples. This work has been supported by the Deutsche Forschungsgemeinschaft (He 1939/11-1).

[1] T. C. Damen, L. Viña, J. E. Cunningham, J. Shah, and L. J. Sham, Phys. Rev. Lett. **67**, 3432 (1991).
[2] S. Bar-Ad and I. Bar-Joseph, Phys. Rev. Lett. **68**, 349 (1992).
[3] A. Vinattieri *et al.*, Solid State Commun. **88**, 189 (1993).
[4] M. Z. Maialle, E. A. de Andrada e Silva, and L. J. Sham, Phys. Rev. B **47**, 15 776 (1993).
[5] L. Muñoz, E. Pérez, L. Viña, and K. Ploog, Phys. Rev. B **51**, 4247 (1995).
[6] T. Amand *et al.*, Phys. Rev. Lett. **78**, 1355 (1997).
[7] R. Spiegel *et al.*, Phys. Rev. B **55**, 9866 (1997).
[8] D. W. Snoke, W. W. Rühle, K. Köhler, and K. Ploog, Phys. Rev. B **55**, 13 789 (1997).
[9] J. Puls, H.-J. Wünsche, and F. Henneberger, Chem. Phys. **210**, 235 (1996); J. Puls, V. V. Rossin, F. Henneberger, and R. Zimmermann, Phys. Rev. B **54**, 4974 (1996).
[10] T. Häupl, H. Nickolaus, F. Henneberger, and A. Schülzgen, Phys. Status Solidi (b) **194**, 219 (1996).
[11] G. L. Bir and G. E. Pikus, *Symmetry and Strain-Induced Effects in Semiconductors* (Wiley, New York, 1975).
[12] J. Puls, F. Henneberger, M. Rabe, and A. Siarkos, J. Cryst. Growth **184/185**, 787 (1998).
[13] H. Nickolaus, M. Lowisch, F. Kreller, and F. Henneberger, J. Cryst. Growth **184/185**, 641 (1998).
[14] M. Wilkinson, F. Yang, E. J. Austin, and K. P. Donnell, J. Phys. Condens. Matter **4**, 8863 (1992).
[15] R. Zimmermann, E. Runge, and F. Grosse, *Proceedings of the 23rd International Conference on the Physics of Semiconductors* (World Scientific, Singapore, 1996).